

Training Stacked Denoising Autoencoders for Representation Learning

Jason Liang
jasonzliang@utexas.edu

Keith Kelly
keith@ices.utexas.edu

Abstract

We implement stacked denoising autoencoders, a class of neural networks that are capable of learning powerful representations of high dimensional data. We describe stochastic gradient descent for unsupervised training of autoencoders, as well as a novel genetic algorithm based approach that makes use of gradient information. We analyze the performance of both optimization algorithms and also the representation learning ability of the autoencoder when it is trained on standard image classification datasets.

I. INTRODUCTION

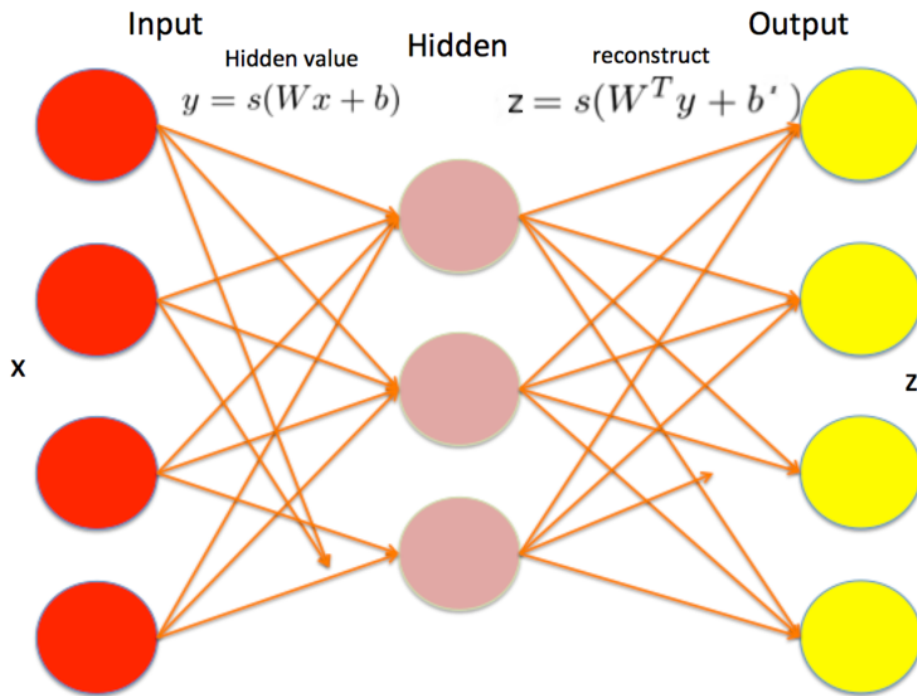


Fig. 1: Overview of an autoencoder and its encoding, decoding stages. The weight matrix of the decoding stage is the transpose of the weight matrix of the encoding stage.

Autoencoders are a method for performing representation learning, an unsupervised pretraining process during which a more useful representation of the input data is automatically determined. Representation learning is important in machine learning since “the performance of machine learning methods is heavily dependent on the choice of data representation (or features) in which they are applied” [1]. For many supervised classification tasks, the high dimensionality of the input data means that the classifier requires an enormous number of training examples in order to generalize well and not overfit. One solution is to use unsupervised pretraining to learn a good representation

for the input data and during actual training, transform the input examples into an easier form for the classifier to learn. Autoencoders are one such representation learning tool.

An autoencoder is a neural network with a single hidden layer and where the output layer and the input layer have the same size. Suppose that the input $x \in \mathbb{R}^m$ (and the output as well) and suppose that the hidden layer has n nodes. Then we have a weight matrix $W \in \mathbb{R}^{m \times n}$ and bias vectors b and b' in \mathbb{R}^m and \mathbb{R}^n , respectively. Let $s(x) = 1/(1 + e^{-x})$ be the sigmoid (logistic) transfer function. Then we have a neural network as shown in Fig. 1. When using an autoencoder to encode data, we calculate the vector $y = s(Wx + b)$; corresponding when we use an autoencoder to decode and reconstruct back the original input, we calculate $z = s(W^T x + b')$. The weight matrix of the decoding stage is the transpose of weight matrix of the encoding stage in order to reduce the number of parameters to learn. We want to optimize W , b , and b' so that the reconstruction is as similar to the original input as possible with respect to some loss function. In this report, the loss function used is the least squares loss: $E(t, z) = \frac{1}{2} \|t - z\|_2^2$, where t is the original input. After an autoencoder is trained, its decoding stage is discarded and the encoding stage is used to transform the training input examples as a preprocessing step. We will refer to the trained encoding stage of the autoencoder as an “autoencoder layer”.

Once an autoencoder layer has been trained, a second autoencoder can be trained using the output of the first autoencoder layer. This procedure can be repeated indefinitely and create stacked autoencoder layers of arbitrary depth. It is been shown that each subsequent trained layer learns a better representation of the output of the previous layer [2]. Using deep neural networks such as stacked autoencoders to do representation learning is also called deep learning, a subfield of machine learning that has received much attention and breakthroughs lately.

For ordinary autoencoders, we usually want that $n < m$ so that the learned representation of the input exists in a lower dimensional space than the input. This is done to ensure that the autoencoder does not learn a trivial identity transformation. However, there also exists an autoencoder variant called *denoising autoencoders* that use a different reconstruction criterion to learn overcomplete representations [2]. In other words, even if $n > m$, a denoising autoencoder can still learn a good representation of the input. This is achieved by corrupting the input image and training the autoencoder to reconstruct the original uncorrupted image. By learning how to denoise, the autoencoder is forced to understand the true structure of input data and learn a good representation of it. Although the loss function $E(t, z)$ for neural networks in general is non-convex, past work has shown that stochastic gradient descent (SGD) is sufficient for most problems. In this report, we will consider training denoising autoencoders with SGD.

In addition, we will examine training autoencoders with other optimization methods such as a genetic algorithm (GA). A GA is a biologically inspired black-box optimization algorithm is capable of optimizing arbitrary non-convex, non-differentiable objective functions. The motivations behind using GAs for training autoencoders are two fold: 1) GAs are a novel approach to optimization of deep neural networks with large number of parameters such as autoencoders. We would like to evaluate the performance of GAs and compare it to SGD. 2) GAs have some advantages over SGD such as being able to escape local optima and easier to parallelize. However GAs also have drawbacks, the main one being its computational complexity over gradient descent. Unlike SGD, a GA must keep a population of individuals and must evaluate each individual for each training example. The computational complexity of a GA is $O(mnd)$ where d is the dimensionality of the individual and optimization problem being solved, n is the population size, and m is the number of training examples; in comparison, the complexity of SGD is $O(md)$. The optimal population size depends on the problem being solved, but in most cases, $n = O(d)$.

We will not just implement a conventional GA (CGA), but also explore hybrid GAs that also make use of gradient information (HGA). The key idea is that with additional gradient information to intelligently update the population every generation, the population size can be kept constant. As a result, the complexity of HGA becomes the same as SGD: $O(md)$, while still retaining the advantages of being more scalable and capable of optimizing arbitrary objective functions.

The rest of this report is as follows: Past research and background literature for autoencoders, dimensionality reduction, genetic algorithms, representation and deep learning can be found in the related work section. The algorithm description section contains more details about how SGD, CGA, and HGA are implemented for autoencoders. The experiments section describes the performance of SGA, CGA, and HGA, as well as the results of training an autoencoder on a handwritten digit image dataset. In the discussion section, we will analyze our findings and report key findings. Finally, in future work, we discuss possible areas of future research.

II. RELATED WORK

Dimensionality reduction of high dimensional data is a common problem in machine learning with many applications. Given input points embedded in high dimensional space, the goal of dimensionality reduction is to

learn a lower dimensional manifold that fits most of the points well. Simpler methods such as principal component analysis (PCA) [3] work by finding the orthogonal directions that best explains the variance of the input data. These directions or “principal components” can be then used to transform the input data by mapping it to coordinates along the principal components. The main drawback of PCA is that it only learn a linear transformation, which means PCA performs poorly when the input data do not lie on a linear manifold (a hyperplane). More sophisticated variants such as kernel PCA [4] deal with nonlinear input by using a nonlinear transformation to map the input data points into a higher dimensional space where they are approximately linear. Other nonlinear manifold learning algorithms include Isomap [5] and t-SNE [6]. These algorithms use heuristics to compute a similarity metric between the input points and then perform multidimensional scaling. Unfortunately, all of these methods mentioned above only work well if the manifold is locally smooth and often degrade in performance for highly varying manifolds [6].

Autoencoders, also known as auto-associators, are a class of feed-forward neural networks that are designed for performing dimensionality reduction and manifold learning [7]. Artificial neural networks are biologically inspired computational structures that are capable of approximating functions of arbitrary shape and dimensionality [8]. Unlike normal neural networks for regression or classification, autoencoders are trained in an unsupervised manner. The weights of an autoencoder can be trained with any optimization algorithm, but the mostly commonly used one is gradient descent, also known as the backpropagation algorithm [9], [10].

Most recent research on autoencoders focus on training them to perform representation learning [1]. Representation learning is a generalization of manifold learning where the goal is not only to discover a lower dimensional substructure, but also to learn a higher dimensional but sparser and more linearly separable representation of the input data. It has been shown that training autoencoders to denoise is one way to learn good representations of the data [2]. Similarly, adding a regularization term that penalizes the Frobenius norm of the Jacobian matrix of the encoder activations is also effective [11]. Furthermore, by stacking autoencoders, it has been shown that the resulting deep neural network is able to overcome the difficulties associated with existing dimensionality reduction methods in learning highly varying manifolds [2], [6].

A related research area to representation learning is deep learning, which explores methods for training deep neural networks such that each subsequent layer learns a higher level representation of the previous layer’s output [12]. It has been shown with each additional layer, the transformed input feature steadily becomes more global and less invariant to local distortions. Compared to shallow neural networks, deep neural networks perform and generalize better on classification tasks, especially for high dimensional inputs. In fact for many difficult datasets, their performance is state of the art by a wide margin [13].

Besides stacked autoencoders, the other two major deep learning architectures are stacked restricted Boltzmann machines (RBMs) [14] and convolutional neural networks (CNNs) [15]. A RBM is an undirected graphical model that is trained to learn the distribution of the input data. The special bipartite structure of the RBM makes Gibbs sampling tractable and gives rise to a fast training algorithm called contrastive divergence [14], [16]. Like autoencoders, RBMs can also be stacked in a similar manner and converted into a deterministic deep neural network [7]. CNNs are a type of deep neural network that is especially designed for processing images and are composed of two main types of layers: convolutional and max pooling. In the convolutional layer, local filters of weights are convolved with the input while in the max pooling layer, the input is down-sampled. CNNs are trained in a supervised manner with backpropagation. Due to the sparsity of the architecture, CNNs can be efficiently trained for input data with millions of dimensions and consequently, achieve state of the art performance in many large scale image classification benchmarks [17]–[19].

A survey of GAs and how they perform optimization can be found in [20]. Much research has been done in applying GAs for optimization of weights in neural networks [21], [22]. There is a small amount of recent work on applying GAs and evolutionary algorithms in general to deep learning [23], [24]. Cantú-Paz discusses methods for parallelizing GAs, which will be essential to scalability when using a GA to train our autoencoder [25].

III. ALGORITHM DESCRIPTION

A. Stochastic Gradient Descent

We start with a random weight matrix W and random biases b and b' . We take a given input x , and feed it forward through the network and compute the error between the target output t and the actual output z . Often we use the squared loss error $E(t, z) = \frac{1}{2} \|t - z\|_2^2$ to determine the difference between the two. In the case of an autoencoder, the target output is the same as the input. If the error is not satisfactory, we can adjust the weight matrix and that biases in order to attempt to learn a better representation of the data. A common method of updating the weight and biases is via backpropagation [9]; when applied to training inputs one at a time, it is also known as stochastic gradient descent (SGD). We will first consider the update for the weights and biases from the last hidden

layer to the output layer with a squared loss error function and derive the updates. We use as an example a simple three layer neural network (input, one hidden and output layer). Some notation is given in Table I.

Symbol	Meaning
E	Error as computed at the output layer
x_j	Node j in the input layer
y_j	Node j in the hidden layer
z_j	Node j in the output layer
n_j	$\sum_{i=1}^n W_{ij} x_i + b_j$
t_j	Target output at node j
W_{ij}^H	Weight i, j from input to hidden layer
W_{ij}^O	Weight i, j from hidden to output layer
$s(x_j)$	$1/(1 + e^{-x_j})$
$b_j^{\{H,O\}}$	Biases for hidden and output layer

TABLE I: Table giving notation for the derivation of updates.

The derivative of the output error E with respect to an output matrix weight W_{ij}^O is as follows.

$$\begin{aligned}
\frac{\partial E}{\partial W_{ij}^O} &= \frac{\partial E}{\partial z_j} \frac{\partial z_j}{\partial W_{ij}^O} \\
&= (z_j - t_j) \frac{\partial s(n_j)}{\partial x_j} \frac{\partial x_j}{\partial W_{ij}^O} \\
&= (z_j - t_j) s(n_j) (1 - s(n_j)) x_i \\
&= (z_j - t_j) z_j (1 - z_j) x_i
\end{aligned} \tag{1}$$

Now that we have the gradient for the error associated to a single training example, we can compute the updates.

$$\begin{aligned}
\delta_j^O &= (z_j - t_j) z_j (1 - z_j) \\
W_{ij}^O &\leftarrow W_{ij}^O - \eta \delta_j^O x_i \\
b_j^O &\leftarrow b_j^O - \eta \delta_j^O
\end{aligned} \tag{2}$$

The computation of the gradient for the weight matrix between hidden layers is similarly easy to compute.

$$\begin{aligned}
\frac{\partial E}{\partial W_{ij}^H} &= \frac{\partial E}{\partial y_j} \frac{\partial y_j}{\partial W_{ij}^H} \\
&= \left(\sum_{k=1}^m \frac{\partial E}{\partial z_k} \frac{\partial z_k}{\partial n_k} \frac{\partial n_k}{\partial y_j} \right) \frac{\partial y_j}{\partial n_j} \frac{\partial n_j}{\partial W_{ij}^H} \\
&= \left(\sum_{k=1}^m (z_k - t_k) (1 - z_k) z_k W_{jk}^O \right) y_j (1 - y_j) x_i
\end{aligned} \tag{3}$$

And then using the computed gradient we can define the updates to be used for the hidden layers

$$\begin{aligned}
\delta_j^H &= \left(\sum_{k=1}^m (z_k - t_k) (1 - z_k) z_k W_{jk}^O \right) y_j (1 - y_j) \\
W_{ij}^H &\leftarrow W_{ij}^H - \eta \delta_j^H x_i \\
b_j^H &\leftarrow b_j^H - \eta \delta_j^H
\end{aligned} \tag{4}$$

In general, for a neural network we may have different output error functions and these will result in different update rules. We will also give the updates for the cross-entropy error function with softmax activation in the final layer. The cross entropy error function is given by $E(x, t) = -\sum_{i=1}^n (t_i \ln z_i + (1 - t_i) \ln(1 - z_i))$ and the softmax function is given by $\sigma(x_j) = e^{x_j} / (\sum_k e^{x_k})$. Following the same procedure as above for computing the gradient and the updates, we find that for hidden/output layer

$$\begin{aligned}
\frac{\partial E}{\partial W_{ij}^O} &= (z_j - t_j)y_i \\
\delta_j^O &= (z_j - t_j) \\
W_{ij}^O &\leftarrow W_{ij}^O - \eta\delta_j^O x_i \\
b_j^O &\leftarrow b_j^O - \eta\delta_j^O.
\end{aligned} \tag{5}$$

We find that the updates for the hidden layer is the same as in the squared error loss function with sigmoid activation. A general overview of the backpropagation algorithm is given by Algorithm 1.

The algorithm and derivations for the autoencoder are a slight variation on the above derivations for a more general neural network. The weight matrix of the output layer (decoding stage) is the transpose of the weight matrix of the hidden layer (encoding stage). Thus $z = s(W^O(W^H x + b) + b')$, $(W^H)^T = W^O$, and $W_{ij}^H = W_{ji}^O$. For training denoising autoencoders in particular, $z = s(W^O(W^H x_{\text{corr}} + b) + b')$, where x_{corr} is a randomly corrupted version of the original input data x_{orig} and the loss function is defined as $E(x_{\text{orig}}, z)$. In other words, we are trying to learn an autoencoder takes in corrupted input and reconstructs the original uncorrupted version. Once we have trained a single autoencoder layer, we can stack another autoencoder layer on top of the first one for further training. This second autoencoder takes the corrupted output of the hidden layer (encoding stage) of the first autoencoder as input and is again trained to minimize the loss function $E(x_{\text{orig}}, z)$.

Algorithm 1 Backpropagation

```

Initialize the weights and biases randomly
for iter = 1, 2, 3... do
  for all Examples  $x$  in training set (randomize) do
     $z \leftarrow$  Feedforward  $x$ 
    Compute output layer  $\delta_j^O$ 
     $W_{ij} \leftarrow W_{ij} - \eta\delta_j^O x_i$ 
     $b_j \leftarrow b_j - \eta\delta_j^O$ 
    for all Layers in reverse order do
      Compute hidden layer delta  $\delta_k^H$ 
       $W_{ij}^H \leftarrow W_{ij}^H - \eta\delta_j^H x_i$ 
       $b_j \leftarrow b_j - \eta\delta_j^H$ 
    end for
  end for
end for

```

After using backpropagation (or a genetic algorithm) to train each of the autoencoder layers, we can then attach an output layer to the autoencoder to be used for classification. At this point we use supervised learning to train the output layer and *fine-tune* the autoencoder layers to produce a classifier based on the autoencoder. When pretraining the autoencoder we train one layer at a time using backpropagation, but during the fine-tuning step we train the entire network via backpropagation, one layer at a time per training image.

B. Genetic Algorithm

As mentioned in the introduction, a genetic algorithm (GA) is a biologically inspired black-box optimization algorithm is capable of optimizing arbitrary non-convex, non-differential objective functions. The GA works by iteratively improving upon a population of candidate solution vectors (also known as individuals) via genetic operations such as selection, mutation, and crossover. The goal is to maximize the fitness of each individual, which is determined by evaluating the individual with some objective function. In the case of autoencoders, the objective function is the reconstruction loss function $E(t, z)$, the individual is a real valued vector that represents the weights (W) and biases (b, b') and the fitness of an individual is simply $1/E(t, z)$. Algorithm 2 shows the pseudocode of a simple conventional genetic algorithm, which we will refer to as CGA.

We will explain step by step what each bold term means and how it affects individuals in the population:

- **Power Scaling:** All individuals in the population are ranked in ascending order according to their fitness. Each individual is assigned a scaled fitness is equal to R^γ where R is the position of the individual

Algorithm 2 Conventional Genetic Algorithm (CGA)

Initialize N individuals randomly by uniformly sampling values from $[-r, r]$
for iter = 1, 2, 3, ..., M , where M is number of training examples **do**
 Evaluate each individual with objective function and assign fitness
 Scale fitness of all individuals, typically with **power scaling** with parameter γ
 Select existing individuals via **roulette selection**
 for every two individuals a and b selected **do**
 Create copies a' and b'
 Perform **uniform mutation** on a' and b' with mutation rate mr and mutation amount ma
 Perform **uniform crossover** using a' and b' with crossover rate cr
 end for
 Replace worst αN ($0 < \alpha < 1$) individuals in population with newly created individuals
end for

within the ranking and γ is a parameter to be tuned. Higher values for γ will create a scaled fitness distribution that favor individuals with higher actual fitness. Thus γ will affect the selection of individuals later and determine how elitist the selection of individuals will be (in other words, how much more likely an individual of higher fitness will be selected).

- **Roulette Selection:** Also known as fitness proportionate selection, roulette selection randomly samples an individual from the population with probability proportional to its scaled fitness. There are many other selection methods such as tournament selection and truncation selection. However, our preliminary experimental results suggest that roulette selection is most appropriate for training weights of autoencoders. The purpose of this operation is to select individuals with good fitness for creating the next generation's population.
- **Uniform Cauchy Mutation:** Each element of the individual (a vector of real numbers) is mutated with probability mr . For each element, we generate a random number between 0 and 1. If this random number is less than mr , we sample a value from a zero-mean Cauchy distribution with standard deviation ma and add that value to the element. The purpose of this operation is to randomly perturb existing individuals and possibly create new ones whose fitness is slightly better.
- **Uniform Crossover:** Each element of the individual is swapped with the same corresponding element of another individual with probability cr . If crossover is performed on two individuals with good fitnesses, there is a chance that the elements of the individuals that are responsible for their high fitnesses might be combined together into a new individual.

Next we will look at HGA, a hybrid GA that combines genetic operators with backpropagation to keep the population size small and remain computationally tractable. The pseudocode for HGA is shown in Algorithm 3 and is based off recent work done by David and Greental [24] on applying GAs to learn stacked autoencoders. The main difference between our HGA and the algorithm described in [24] is that we use roulette selection instead of truncation selection and uniform Cauchy mutation instead of mutating weights to zero.

Algorithm 3 Hybrid Genetic Algorithm (HGA)

Initialize N individuals randomly by uniformly sampling values from $[-r, r]$
for iter = 1, 2, 3, ..., M , where M is number of training examples **do**
 Evaluate each individual with objective function and assign fitness
 Scale fitness of all individuals, typically with **power scaling** with parameter γ
 Perform *backpropagation on top βN ($0 < \beta < 1$) individuals with highest fitness*
 Select existing individuals via **roulette selection**
 for every two individuals a and b selected **do**
 Create copies a' and b'
 Perform **uniform mutation** on a' and b' with mutation rate mr and mutation amount ma
 Perform **uniform crossover** using a' and b' with crossover rate cr
 end for
 Replace worst αN ($0 < \alpha < 1$) individuals in population with newly created individuals
end for

The key idea of performing backpropagation is that it assists the mutation operator in moving the individuals

towards regions of high fitness. While the mutation operator perturbs individuals randomly, backpropagation will always follow the gradient. This distinction is significant in high dimensional spaces, as the mutation operator will require a large population size to work optimally, while backpropagation does not. Instead, the mutation operator serves a secondary role of helping the individuals to escape from a local optima through random perturbations. Preliminary results show that compared to CGA with the same population size, HGA performs significantly better. Furthermore, the performance of HGA does not degrade significantly with smaller population sizes, even when using an extremely small population size of 2.

IV. EXPERIMENTAL RESULTS

For the following experiments, we train our autoencoder over the MNIST handwritten digit dataset. The MNIST dataset is composed of 60000 training images and 10000 testing images. Each image is in greyscale, is 28 by 28 pixels in size, and has a corresponding label ranging from 0 to 9. Thus, the input vector for our autoencoder has 784 dimensions. We also make use of the denoising criterion mentioned in [2], and for each training image, randomly corrupt it by setting each pixel to zero with probability 0.25. All experiments were ran on a TACC Stampede cluster with 16 cores.

A. Stochastic Gradient Descent

We first analyze how the number of threads affects the rate at which reconstruction error decreases for SGD. We train a single autoencoder layer with 500 hidden nodes for 15 iterations over 5000 training images. An iteration involves going through all training images and for each image, use SGD to update the weight matrix. We initialize the weights of the autoencoder randomly by sampling from the interval $[-1/\sqrt{\text{FANIN}}, 1/\sqrt{\text{FANIN}}]$, where FANIN is the dimensionality of the input. Fig. 2 shows the relationship between reconstruction error, total time elapsed, and the number of threads used. Regardless of the number of threads, the reconstruction error decreases sharply in the first few iterations before flattening out to around the same value after 15 iterations. The rate at which error decreases is significantly faster for 4 and 8 threads when compared to just using one. Nonetheless, the speedup is not linear (using 16 threads is actually marginally slower than using 8) and is due to two reasons: 1) Possible cache conflicts as each thread read and writes to different locations in the weight matrix. 2) All the steps for backpropagation/SGD, described in Algorithm 1, must be done sequentially. Parallelization can only be done within each step and incurs an overhead cost.

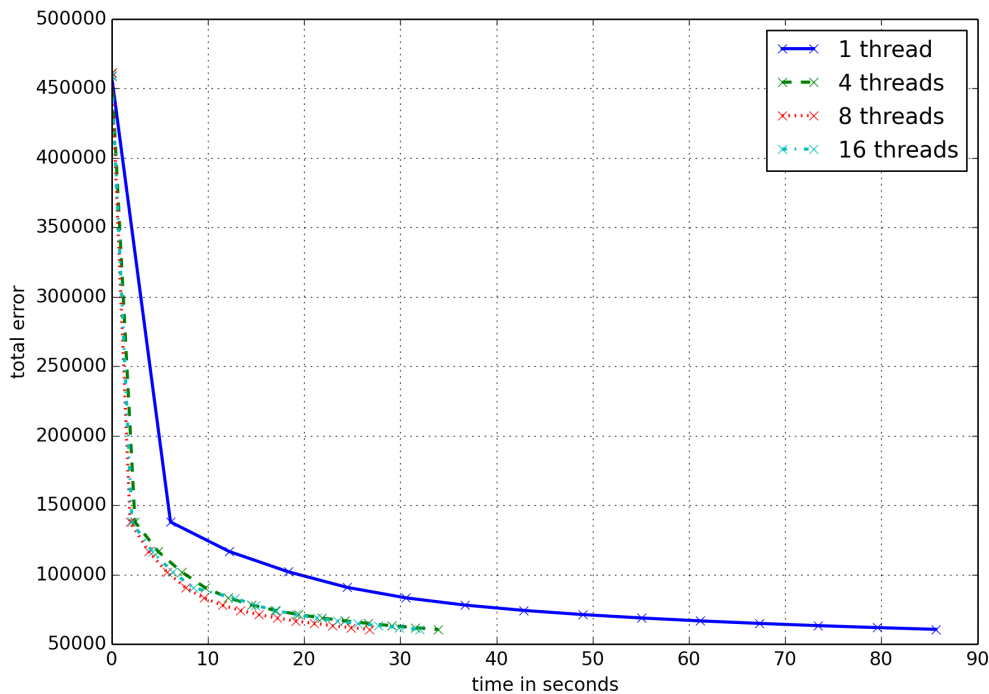


Fig. 2: Performance results on a single autoencoder layer with 500 hidden nodes and trained for 15 iterations. Plot shows time elapsed versus total training error over 5000 images for 1, 4, 8, and 16 threads.

We note that the steps of backpropagation can only be done in sequence; thus we can only parallelize the operations done within each step. The three major operations which benefit from parallelization are computing the matrix-vector products $W^H x$ and $W^O y$, computing δ_j^O and δ_j^H , and updating the entries of the weight matrices with the gradient. For performance reasons we don't store W^O separately; instead we access W^H with transposed indexes when decoding, calculating δ_j^O , and applying the gradient update.

The most expensive parts of the backpropagation algorithm are computing the forward activations of the network and updating the weight matrices for the network. Computing the forward propagation requires performing a matrix-vector multiplication at each layer of the network. The size of that matrix depends on the input and output sizes of that layer. Thus if we have a network with N layers and the sizes of each of those layers is n_i , then we have N matrix-vector multiplications of size $n_{i-1} \times n_i$. Updating the weights also has complexity based on the size of the matrix since it requires updating all the entries of the matrix at each iteration.

To improve the performance of these two expensive steps, we parallelized them first using OpenMP and then later parallelized the matrix-vector products using OpenBLAS. Parallelization of these two steps is fairly straightforward and we give some results on scaling in Figs. 3, 4, and 5.

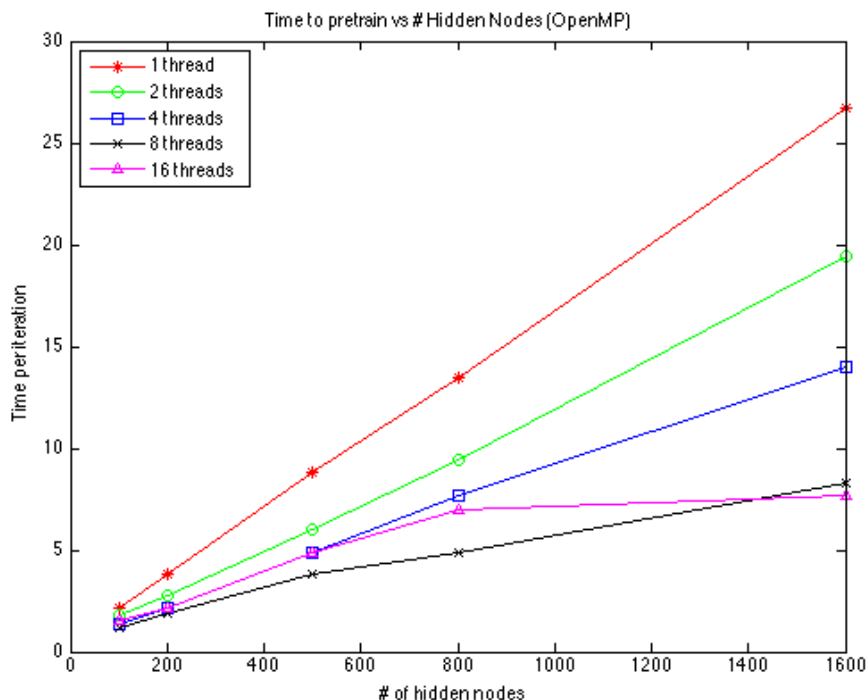


Fig. 3: Time per iteration versus the number of threads and hidden nodes. We parallelize with our own OpenMP implementation and use 5000 training images.

In Fig. 3 we give the performance of training the autoencoder using SGD for different numbers of hidden nodes and different numbers of threads using our own parallel implementation. In Fig. 4 we give the performance of training the autoencoder using SGD for different numbers of hidden nodes and different numbers of threads using OpenBLAS for parallelization of the matrix-vector multiplies and matrix-transpose-vector multiplies. The weight updates are not able to be done in OpenBLAS, and so we continue to do that using OpenMP. We consider the relative performance of these two methods in Fig. 5.

We note that Figs. 3 and 4 show similar scaling, though in most cases the OpenBLAS version outperforms our own implementation. However, for small numbers of nodes, OpenBLAS does not perform well with many threads. We generally get better performance with a greater number of threads, but with a large number of threads we do not see improvement until the problem size increases and becomes large enough. We do not achieve linear scaling (i.e. twice as many threads does not result in the algorithm running twice as fast), since not all parts of the algorithm can be parallelized.

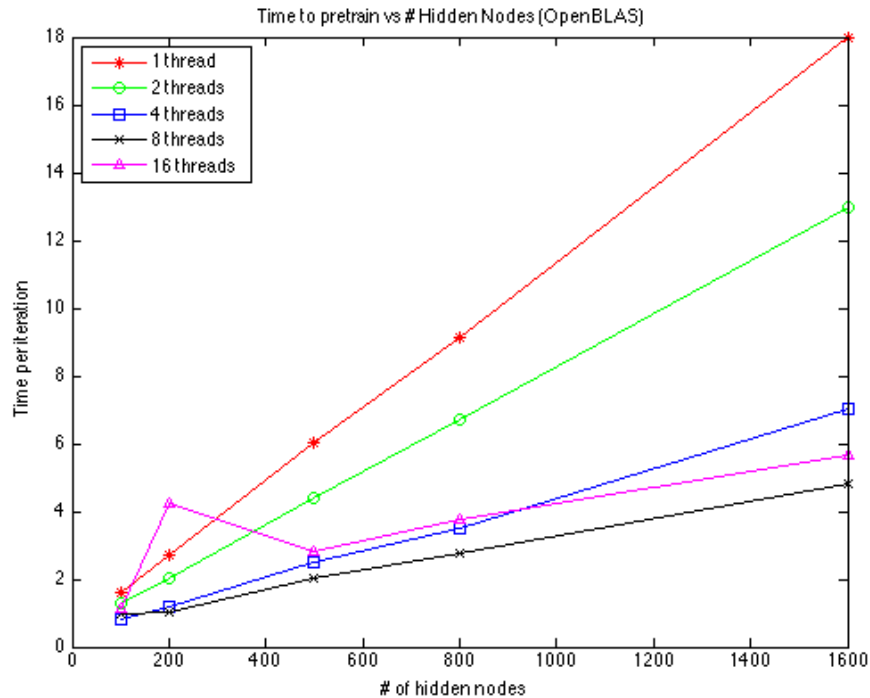


Fig. 4: Time per iteration versus the number of threads and hidden nodes. We parallelize with OpenBLAS and we use 5000 training images.

B. Visualization of Trained Weights and Reconstructed Images

Next, in Fig. 6, we visualize the filters that are learned by training an autoencoder layer with 500 hidden nodes over all 60000 training images. The filter for each hidden node is a row vector of the weight matrix and indicates which aspects of the input the hidden unit is sensitive to. Since each row in the weight matrix is the same dimensionality as the input, we can visualize it as a 28 by 28 pixel image. The filters are not identical to the input images, but do show some similarity to them. In Fig. 7, we visualize the reconstructed digits when given noisy test digits as input. The reconstructed outputs for most of the input images are easily recognizable as digits, which indicates that the autoencoder is indeed denoising and learning a good representation of the images.

To further demonstrate the reconstruction capabilities of the autoencoder, we trained the autoencoder on corrupted or otherwise altered digits. In particular, we test the reconstruction on *bg-rand*, which is generated from the MNIST dataset, except that a random background is added. In *bg-img*, each image is given a background randomly selected from one of twenty images downloaded from the internet. In *rot*, the digits are simply rotated by some random angle. These alterations to the images make the classification task more difficult. Indeed the digits are very difficult to identify, but the autoencoder creates an easier to identify representation, even to the human eye. We show also in Fig. 7 the reconstructed images from the *bg-img* and *rot* datasets. Note that the images in the *bg-rand* and *bg-img* datasets are rotated, but they are all rotated in the same way.

Finally we evaluate the classification accuracy of a deep neural network that has multiple stacked denoising autoencoders. We train 3 stacked autoencoder layers, each with 1000 hidden units, and using noise levels 0.1, 0.2, and 0.3 respectively. Each layer is trained for 15 iterations with a learning rate of 0.001. After the unsupervised pretraining, a conventional feed-forward network with 1000 input units, 500 hidden units and 10 outputs is connected to the hidden units of the last autoencoder layer. This conventional network is then trained for 30 iterations (learning rate 0.1) in a supervised manner, where the target t is the indicator vector representation of the training label. Our final classification accuracy is 98.04%. In comparison, the best reported accuracy achieved with a SVM with RBF kernel is 98.60% [2].

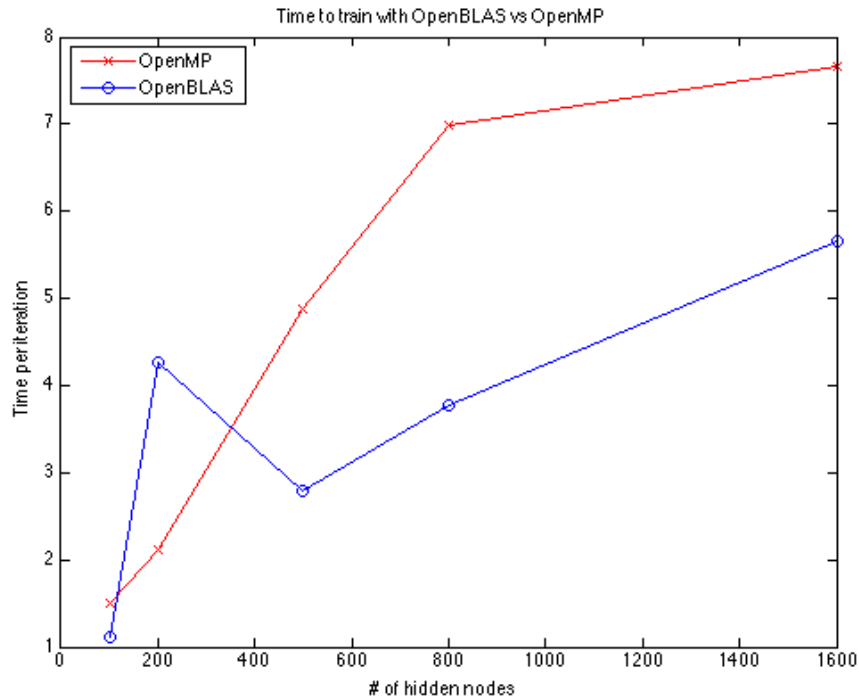


Fig. 5: Time per iteration versus parallelization technique and hidden nodes. We use 16 threads here.

C. Representation Learning for Supervised Classification

Recall that one of the main reasons for using an autoencoder is to determine a more useful representation of the data for other tasks, for example in a classification task. To this end, we constructed and trained (15 iterations) an autoencoder with just a single layer and 1000 hidden units and used it to create a more useful representation of the digits in the MNIST dataset. After this more useful representation is constructed, we can then use the output from the autoencoder as input to another type of classification algorithm. Since the autoencoder produces a better representation of the data, we expect that given the encoded data, the other classification algorithms should perform better. The results of these experiments is given in Table. II.

To test this, we used liblinear [26] to attempt to train a model and then predict on a test set for both the original and encoded datasets. With the original data, liblinear gives an accuracy of 91.68% on the test set when using the default parameters. However, the encoded data from the trained autoencoder gives an accuracy of 97.07%. This is a nontrivial improvement in the classification accuracy. Thus, the autoencoder has created a better representation of the data which made it easier for liblinear to classify. This verifies that the autoencoder is doing what it is expected to do.

Similarly, we performed the same experiment as above, except in this case we used libsvm [27] with an RBF kernel and all the default parameters. Without encoding the data first, we get an accuracy of 94.46%, but using the encoded data gives a prediction accuracy of 95.48%. As above, the encoded data allows libsvm better classify the data. We should note that our accuracy is not as good as the one reported earlier as we did not tune the hyperparameters (C and kernel width) of the SVM classifier.

Using logistic regression to perform the classification, we experienced similar results. Again we use liblinear with all default options except selecting logistic regression. Using the original MNIST data, this algorithm achieved an accuracy of 91.82% while with the encoded data we achieved an accuracy of 96.86%.

We performed the same experiments on the *bg-rand*, *bg-img* and *rot* datasets as well. Across the board we see similar results. The encoding does not have much of an effect on the ability of kernel SVM to classify the data, but for linear SVM and logistic regression, using the autoencoder always results in the classifier improving it's accuracy.

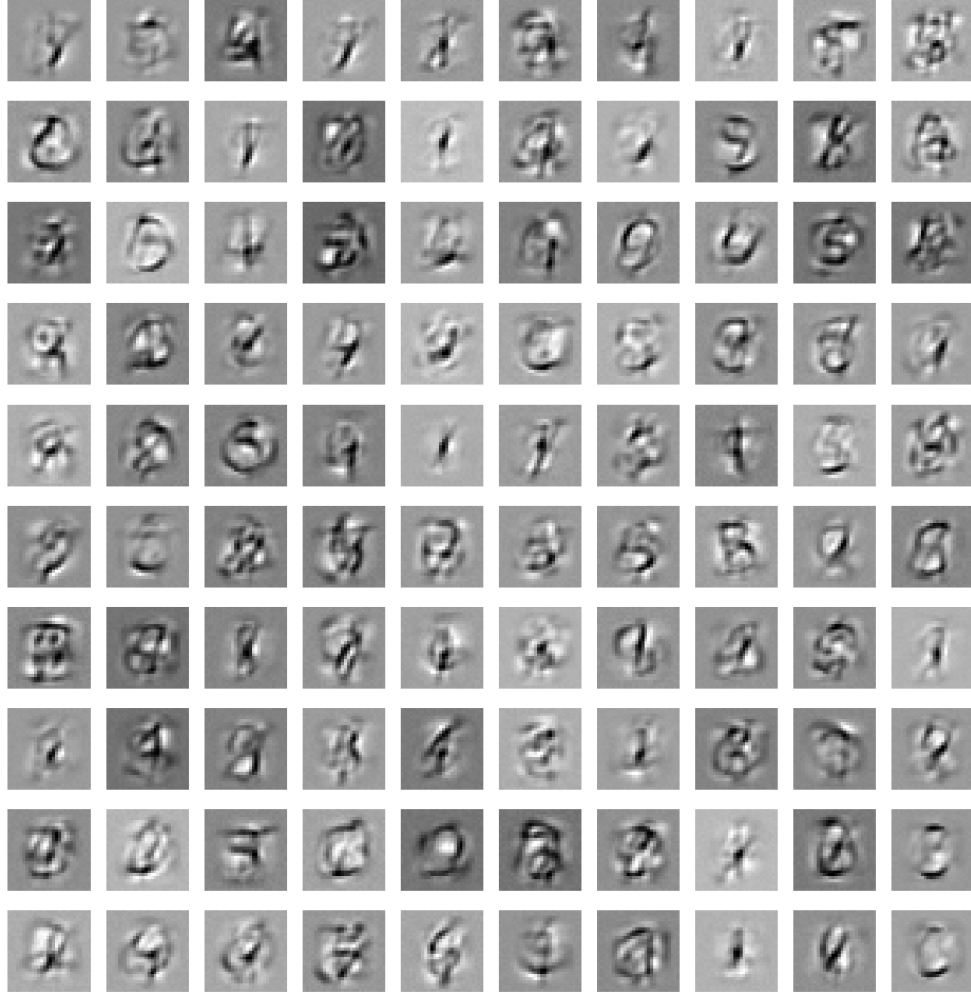


Fig. 6: Visualization of the filters of the first 100 hidden nodes in an denoising autoencoder trained over all 60000 images.

Dataset	Data	Linear SVM	Kernel SVM (RBF)	Logistic Regression
MNIST	Original	91.68%	94.46%	91.82%
	Encoded	97.07%	95.48%	96.86%
mnist-bg-rand	Original	58.975%	83.875%	65.5917%
	Encoded	81.675%	83.6583%	83.825%
mnist-bg-img	Original	69.25%	76.4667%	71.6333%
	Encoded	78.4333%	72.8417%	78.1333%
mnist-rot	Original	11.204%	13.328%	11.868%
	Encoded	18.428%	14.378%	18.78%

TABLE II: Summary of the results of running different classification algorithms on the raw MNIST data and on the output from a trained autoencoder. We see in nearly all cases that using the encoded data produces a better result.

D. Genetic Algorithms

For all of the following experiments, we train a single autoencoder layer with 1000 hidden units and cycle through 1000 training digits for 15 iterations. The default hyperparameters for CGA and HGA are listed in Table. III. To parallelize the GA, we modified the mutation and crossover operators to support multiple threads. Because mutation and crossover modifies each element of the individual independently, no locking is required. The computation of an individual's fitness is already parallelized since it reuses the same code from SGD for determining the least squares loss. The remaining operations of the GA does not need parallelization since they are computationally cheap.

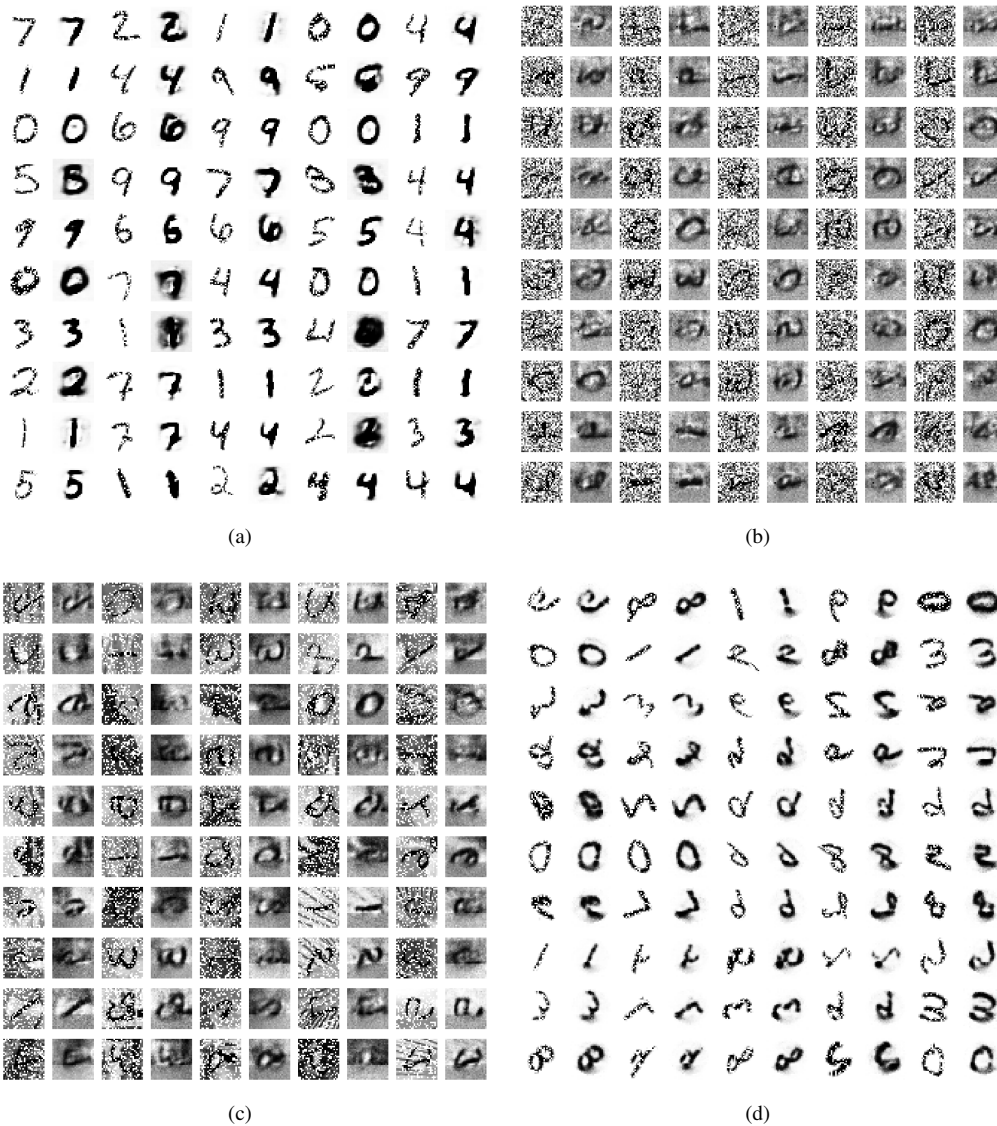


Fig. 7: Reconstructions of corrupted digits from the (a) MNIST dataset (b) bg-rand dataset, (c) bg-img dataset, and (d) rot dataset

In Fig. 8, we compare the performance of SGD, HGA (uses backpropagation to update the best individuals in the population), and CGA (does not use any gradient information). SGD is the fastest by roughly a factor of two when compared to HGA, while CGA is somewhere in between. However, HGA is able to achieve the lowest reconstruction error (8709 vs SGD's 9427). CGA performed the worst out of all three algorithms, having a reconstruction error that is three times larger than that of the other algorithms. The hyperparameters for HGA and CGA are hand tuned and not necessary optimal. However, we believe that with properly tuned hyperparameters, HGA might be competitive with SGD for both final reconstruction error and performance time.

Next in Fig. 9, we examine the scalability of HGA. HGA shows roughly 3x speedup when using 4 threads, 5x speedup when using 8 threads, and 6x speedup when using 16 threads. The performance improvement versus the number of threads is sub-linear and can be attributed to two main causes: 1) Cache conflicts when performing mutation and crossover due to multiple threads writing and reading different memory locations, 2) The sequential nature of backpropagation, which HGA utilizes to help optimize the weights. However, HGA does seem to have moderately better scalability than our parallel implementation of SGD. This is attributable to the fact that the mutation and crossover operators are very straightforward to parallelize and scale in performance very well.

Hyperparameter	Value
Mutation Rate mr	0.0001
Mutation Amount ma	$0.1r$
Crossover Rate cr	0.5
Population Size N	2
Replacement Fraction α	0.5
Initial Value Range r	$1/\sqrt{FANIN}$
Power Scaling Parameter γ	1.0
Backpropagation Fraction β (HGA only)	0.5

TABLE III: List of hyperparameters for CGA and HGA. FANIN is input dimensionality of autoencoder layer.

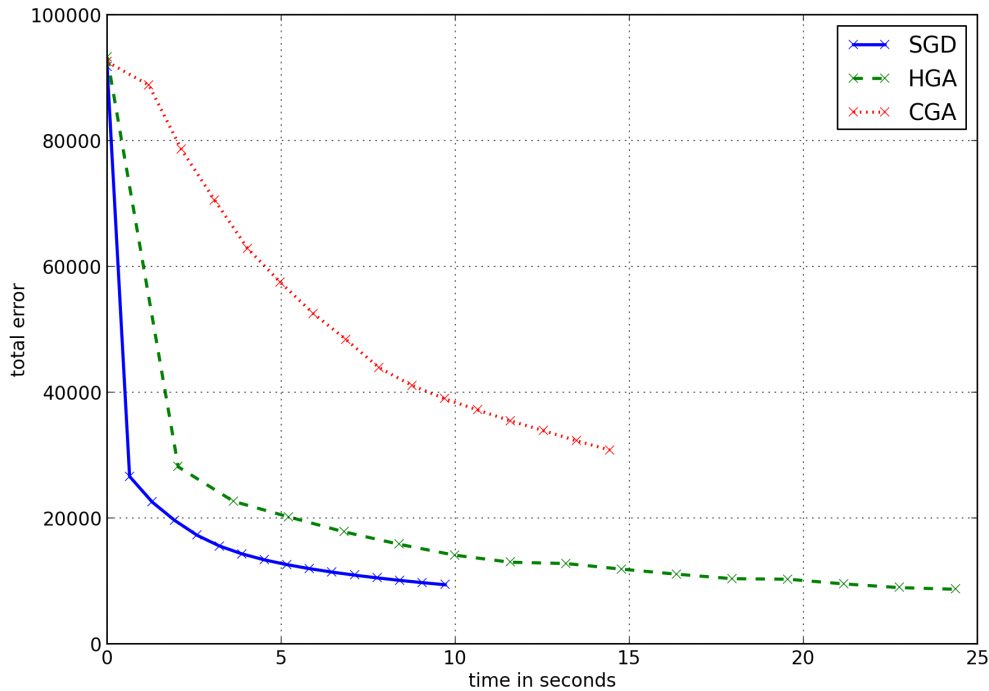


Fig. 8: Comparison of the performance of SGD, HGA, and CGA. SGD is fastest, while HGA achieves the lowest reconstruction error. HGA and CGA uses a default population size of 2 and all three algorithms cycle through 1000 training images for 15 iterations.

In Fig. 10, the performance of HGA versus the number of threads and number of hidden units in autoencoder layers is visualized for both a population size of 50 and the default size of 2. As we can see, the HGA’s performance scales linearly with the number of hidden units and that this relationship holds even when the population size is increased to 50. Interestingly, the performance when using 8 or 16 threads is not distinguishable for small numbers of hidden units. This is probably due to the computational overhead that result from creating additional threads.

Finally, in Fig. 11, we plot the performance of CGA and HGA for population sizes of 2, 4, 8, 16, and 32. All other hyperparameters remain the same for both HGA and CGA. As we can see, larger populations does lead to a noticeable improvement in the final reconstruction error, but at a cost of increased running time that is linear in the population size. For each fixed population size, HGA performs significantly better than CGA, with a final construction error is roughly three to five times lower. However for a given population size, HGA does take 40% to 50% longer to finish; this is attributable to the fact that CGA does not perform backpropagation, which takes additional time.

V. DISCUSSION

The experimental results demonstrate the importance of learning a better representation of the data for the classification algorithms given. While the kernel SVM performed comparably with and without the improved representation of the data, it is also much more expensive than the linear SVM or logistic regression methods. Thus the trade off becomes whether to use a more expensive classifier, or to learn a better representation and then

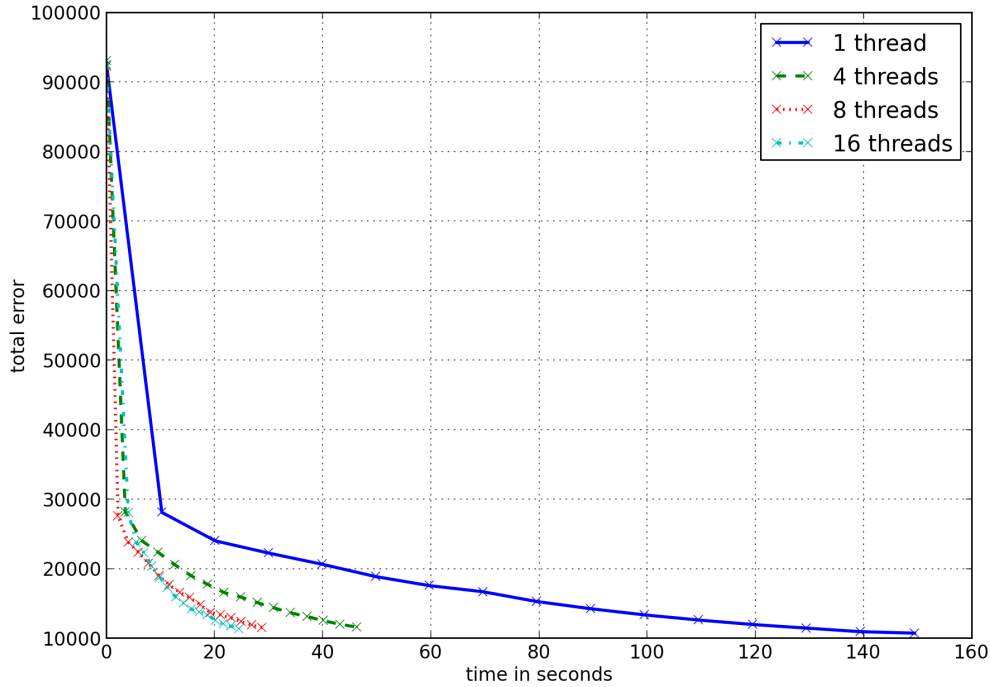


Fig. 9: Performance of HGA for 1, 4, 8, and 16 threads with a population size of 2 and 1000 training images.

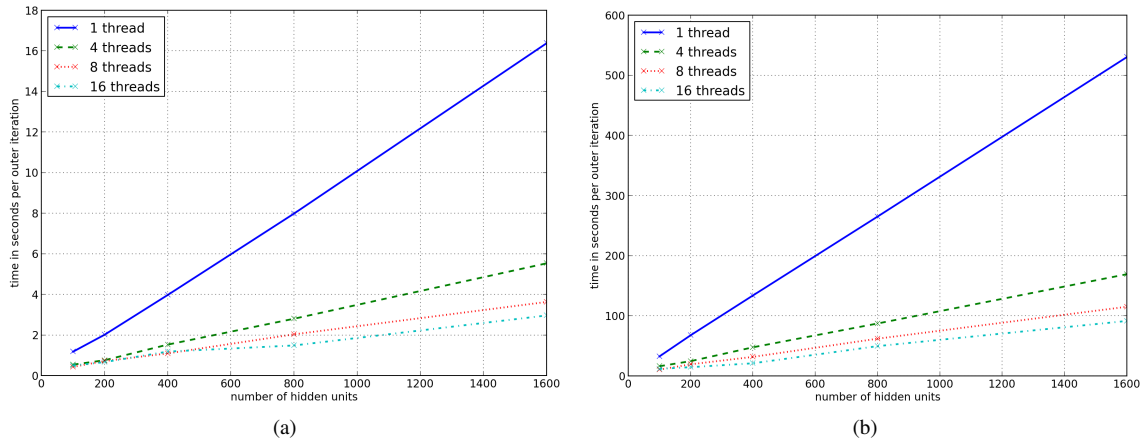


Fig. 10: Comparison of performance versus number of threads and number of hidden units in autoencoder layer for HGA with population size (a) 2 and (b) 50.

use a cheaper classifier. It is also important to consider that the autoencoder combined with a simple classifier performed better than the kernel SVM in several cases.

As we saw in the results section, SGD is the fastest method for training the autoencoder, in terms of wall-time. That is, to achieve a given error rate, using SGD will be faster than HGA or CGA in terms of time (as opposed to number of iterations). This might suggest that SGD is the preferred method for training an autoencoder, but it does not come without drawbacks. In terms of the number of iterations to achieve a given error rate, we saw that HGA performed the best, with SGD second and CGA last. This is important because of how the methods scale. SGD scales decently with respect to increasing number of threads, but the genetic algorithms demonstrate better scaling properties, being closer to linear in their scaling. Furthermore, HGA is able to achieve the lowest error rate of any of the methods considered. Reconstruction error is an indication of how well the autoencoder encodes

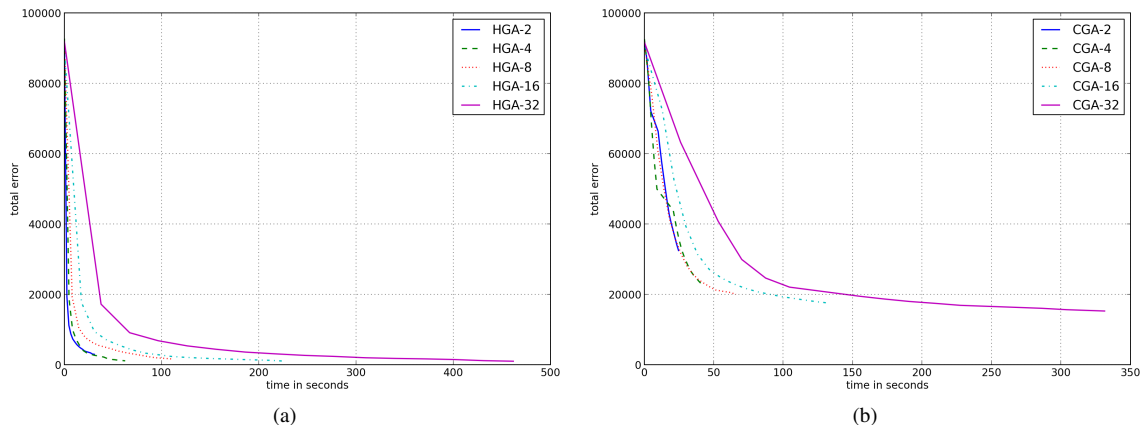


Fig. 11: Comparison of performance for (a) HGA and (b) CGA with population sizes of 2, 4, 8, 16, and 32. HGA performs significantly better than CGA in terms of final reconstruction error.

(and decodes) the input; by this metric HGA is a better optimization method than SGD.

However, genetic algorithms have many parameters that need to be tuned and are problem dependent. In contrast, SGD has only one: the learning rate. Consequently it can sometimes be difficult to get GAs to converge at all or at a reasonable rate without knowing the correct parameters. Thus it may be interesting to consider a meta-optimization of the parameters for a genetic algorithm, so that this tuning may be done automatically.

VI. FUTURE WORK

As mentioned above, genetic algorithms are sensitive to their parameters. Consequently, much time and effort may be required in order to determine the optimal parameters and achieve good convergence performance. Without the correct parameters, the genetic algorithm may not converge to a solution at all or may converge very slowly. A technique known as meta-optimization could be used to automatically determine the correct parameters for performing the optimization. Grefenstette discusses this meta-optimization over six possible parameters for the genetic algorithm [28]. Finding the best possible parameters may result in better convergence for our genetic algorithms in both rate of error decrease and minimum error achieved.

Another direction to consider is the adaptive selection of crossover or mutation probability during the training of the autoencoder. This so-called adaptive genetic algorithm reaches the global optimum for a cost function much more quickly than a standard genetic algorithm [29]. This adaptive method could be applied to either CGA or to HGA and further improve its performance.

Our experiments and results are based on shared memory, single machine parallelism. An interesting future topic to explore is expanding the methods we considered to more cores and more machines. Expanding to more cores is a trivial extension requiring just the appropriate multi-core hardware with more than 16 processor cores on a node. Expanding what we have done to a distributed setting would require more work, and rewriting much of the code. Stochastic gradient descent has been shown to be a scalable method for a distributed setting (see, for example [30]) so it seems reasonable that it should scale in this application as well. Genetic algorithms have also been shown to demonstrate good scaling properties for distributed computations [31].

VII. CONCLUSION

We have implemented stacked denoising autoencoders and shown that it achieves accuracy comparable to state of the art classifiers like a SVM with RBF kernel. We also have shown that our autoencoder layers are learning good representations and are capable of denoising and reconstructing the input with little error. These learned representations improve the ability of other classification algorithms to correctly classify the data. We find that SGD scales well with increasing number of hidden units and with increasing number of threads. Lastly, we discovered that HGA, a genetic algorithm that makes use of gradient information, is competitive with SGD, and scales just as well if not better with the size of the autoencoder and number of threads.

REFERENCES

- [1] Yoshua Bengio, Aaron C. Courville, and Pascal Vincent. Unsupervised feature learning and deep learning: A review and new perspectives. *CoRR*, abs/1206.5538, 2012.
- [2] Pascal Vincent, Hugo Larochelle, Isabelle Lajoie, Yoshua Bengio, and Pierre-Antoine Manzagol. Stacked denoising autoencoders: Learning useful representations in a deep network with a local denoising criterion. *The Journal of Machine Learning Research*, 11:3371–3408, 2010.
- [3] Svante Wold, Kim Esbensen, and Paul Geladi. Principal component analysis. *Chemometrics and intelligent laboratory systems*, 2(1):37–52, 1987.
- [4] Bernhard Schölkopf, Alexander Smola, and Klaus-Robert Müller. Kernel principal component analysis. In *Artificial Neural Networks—ICANN'97*, pages 583–588. Springer, 1997.
- [5] Joshua B Tenenbaum, Vin De Silva, and John C Langford. A global geometric framework for nonlinear dimensionality reduction. *Science*, 290(5500):2319–2323, 2000.
- [6] Laurens Van der Maaten and Geoffrey Hinton. Visualizing data using t-sne. *Journal of Machine Learning Research*, 9(2579-2605):85, 2008.
- [7] Geoffrey E Hinton and Ruslan R Salakhutdinov. Reducing the dimensionality of data with neural networks. *Science*, 313(5786):504–507, 2006.
- [8] Simon Haykin. Neural networks: A comprehensive foundation. *Neural Networks*, 2(2004), 2004.
- [9] Robert Hecht-Nielsen. Theory of the backpropagation neural network. In *Neural Networks, 1989. IJCNN., International Joint Conference on*, pages 593–605. IEEE, 1989.
- [10] Léon Bottou. Stochastic gradient learning in neural networks. In *Proceedings of Neuro-Nîmes 91*, Nîmes, France, 1991. EC2.
- [11] Salah Rifai, Pascal Vincent, Xavier Muller, Xavier Glorot, and Yoshua Bengio. Contractive auto-encoders: Explicit invariance during feature extraction. In *Proceedings of the 28th International Conference on Machine Learning (ICML-11)*, pages 833–840, 2011.
- [12] Yoshua Bengio. Learning deep architectures for ai. *Foundations and trends® in Machine Learning*, 2(1):1–127, 2009.
- [13] Jürgen Schmidhuber. Deep learning in neural networks: An overview. *arXiv preprint arXiv:1404.7828*, 2014.
- [14] Geoffrey Hinton, Simon Osindero, and Yee-Whye Teh. A fast learning algorithm for deep belief nets. *Neural computation*, 18(7):1527–1554, 2006.
- [15] Yann LeCun and Yoshua Bengio. Convolutional networks for images, speech, and time series. *The handbook of brain theory and neural networks*, 3361, 1995.
- [16] Geoffrey E. Hinton, Simon Osindero, and Yee-Whye Teh. A fast learning algorithm for deep belief nets. *Neural Comput.*, 18(7):1527–1554, July 2006.
- [17] Dan Ciresan, Ueli Meier, Jonathan Masci, and Jürgen Schmidhuber. A committee of neural networks for traffic sign classification. In *Neural Networks (IJCNN), The 2011 International Joint Conference on*, pages 1918–1921. IEEE, 2011.
- [18] Alex Krizhevsky, Ilya Sutskever, and Geoffrey E Hinton. Imagenet classification with deep convolutional neural networks. In *Advances in neural information processing systems*, pages 1097–1105, 2012.
- [19] Ian J Goodfellow, Yaroslav Bulatov, Julian Ibarz, Sacha Arnoud, and Vinay Shet. Multi-digit number recognition from street view imagery using deep convolutional neural networks. *arXiv preprint arXiv:1312.6082*, 2013.
- [20] Mandavilli Srinivas and Lalit M Patnaik. Genetic algorithms: A survey. *Computer*, 27(6):17–26, 1994.
- [21] Faustino Gomez, Jürgen Schmidhuber, and Risto Miikkulainen. Efficient non-linear control through neuroevolution. In *Machine Learning: ECML 2006*, pages 654–662. Springer, 2006.
- [22] Dario Floreano, Peter Dürri, and Claudio Mattiussi. Neuroevolution: from architectures to learning. *Evolutionary Intelligence*, 1(1):47–62, 2008.
- [23] Jan Koutník, Juergen Schmidhuber, and Faustino Gomez. Evolving deep unsupervised convolutional networks for vision-based reinforcement learning. In *Proceedings of the 2014 conference on Genetic and evolutionary computation*, pages 541–548. ACM, 2014.
- [24] Omid E David and Iddo Greental. Genetic algorithms for evolving deep neural networks. In *Proceedings of the 2014 conference companion on Genetic and evolutionary computation companion*, pages 1451–1452. ACM, 2014.
- [25] Erick Cantú-Paz. A survey of parallel genetic algorithms. *Calculateurs parallèles, reseaux et systems repartis*, 10(2):141–171, 1998.
- [26] Rong-En Fan, Kai-Wei Chang, Cho-Jui Hsieh, Xiang-Rui Wang, and Chih-Jen Lin. Liblinear: A library for large linear classification. *The Journal of Machine Learning Research*, 9:1871–1874, 2008.
- [27] Chih-Chung Chang and Chih-Jen Lin. Libsvm: a library for support vector machines. *ACM Transactions on Intelligent Systems and Technology (TIST)*, 2(3):27, 2011.
- [28] J.J. Grefenstette. Optimization of control parameters for genetic algorithms. *Systems, Man and Cybernetics, IEEE Transactions on*, 16(1):122–128, Jan 1986.
- [29] M. Srinivas and L.M. Patnaik. Adaptive probabilities of crossover and mutation in genetic algorithms. *Systems, Man and Cybernetics, IEEE Transactions on*, 24(4):656–667, Apr 1994.
- [30] Martin Zinkevich, Markus Weimer, Lihong Li, and Alex J. Smola. Parallelized stochastic gradient descent. In J.D. Lafferty, C.K.I. Williams, J. Shawe-Taylor, R.S. Zemel, and A. Culotta, editors, *Advances in Neural Information Processing Systems 23*, pages 2595–2603. Curran Associates, Inc., 2010.
- [31] Theodore C. Belding. The distributed genetic algorithm revisited. In *Proceedings of the Sixth International Conference on Genetic Algorithms*, pages 114–121, 1995.